Master's Thesis

Interactions of PP2A inhibitor proteins with PP2A regulatory subunits

Pekka Roivas

University of Jyväskylä

Department of Biological and Environmental Science

Cell- and molecular biology

02 June 2020

UNIVERSITY OF JYVÄSKYLÄ, Faculty of Mathematics and Science
Department of Biological and Environmental Science
Cell- and molecular biology

Pekka Roivas:	Interactions of PP2A inhibitor proteins with PP2A regulatory subunits
MSc thesis:	35 p., 1 appendix (1 p.)
Supervisors:	Ph.D Ulla Pentikäinen and Ph.D Jari Ylänne
Reviewers:	Ph.D Tatu Haataja and Ph.D Perttu Permi
June 2020	

Keywords: ARPP16, ARPP19, CIP2A, ENSA, Phosphatase, Phosphomimic

Phosphatases are important factors in cellular regulation. Protein phosphatase 2A (PP2A) is one of these regulators and its functions are related in activation of cell cycle. When the normal functions of PP2A are disturbed it can lead to various diseases, including cancer. This disturbance can be caused by various protein inhibitors. Inhibitor proteins from cAMP regulated phosphoprotein/α-endosulfin family and Cancerous Inhibitor of PP2A (CIP2A) has already been confirmed as PP2A inhibitors, but their inhibition mechanisms are mostly unknown. PP2A is a heterotrimeric protein that consists of scaffolding, regulatory and catalytic subunit. At least 23 different isoforms have been discovered between its regulatory B subunits. In this study, the binding of these inhibitor proteins is measured with three different PP2A B subunit isoforms B56γ, B56δ and B56ε. To activate the binding capabilities of cAMP regulated phosphoprotein/α-endosulfin family inhibitors, two different phosphomimicking mutants for each inhibitor was also tested. These B56 isoforms were first expressed and purified, and then their protein-protein interaction with these inhibitor proteins was studied using microscale thermophoresis method. The results showed that wild type cAMP regulated phosphoprotein/α-endosulfin family inhibitors bound to all these subunits. Binding of CIP2A domains was varying. cAMP-regulated phosphoprotein 19 kDa (ARPP19) and cAMP-regulated phosphoprotein 16 kDa (ARPP16) bearing phosphomimicking mutations binds to B56 isoforms, whereas alpha-endosulfine (ENSA) phosphomimicking mutation did not show binding.

JYVÄSKYLÄN YLIOPISTO, Matemaattis-luonnontieteellinen tiedekunta
Bio- ja ympäristötieteiden laitos
Solu- ja molekyylibiologia

Pekka Roivas: PP2A:n inhibiittoriproteiinien vuorovaikutus PP2A:n säätelijä alayksikön kanssa

Pro gradu -tutkielma: 35 s., 1 liite (1 s.)
Työn ohjaajat: FT Ulla Pentikäinen ja FT Jari Ylänne
Tarkastajat: FT Tatu Haataja ja FT Perttu Permi
Kesäkuu 2020

Hakusanat: ARPP16, ARPP19, CIP2A, ENSA, Fosfataasi, Fosfomatkija

Fosfataasit ovat tärkeitä solun sisällä tapahtuvan säätelyn kannalta. Proteiinifosfataasi 2A (PP2A) on yksi näistä säätelijöistä ja sen normaali toiminta liittyy solusyklin aktivointiin. Kun PP2A:n normaalia toimintaa häiritään, voi sen seurauksena ilmetä erilaisia sairauksia, kuten syöpää. PP2A:n toimintaa estävien inhibiittoriproteiinien on huomattu olevan mahdollinen syy tähän häiriöön. Inhibiittoriproteiinien, kuten fosfoproteiini/α-endosulfiini perheen proteiinien ja Cancerous Inhibitor of PP2A (CIP2A) on huomattu estävän PP2A:ta, mutta niiden sitoutumismekanismeista PP2A:n tiedetään vähän. PP2A on heterotrimeerinen proteiini ja se koostuu tuki-, säätelijä- ja katalyyttisestä alayksiköstä. PP2A:n säätelyalayksikkö B:n sisällä on tavattu ainakin 23 erilaista isoformia. Tässä tutkimuksessa inhibiittoriproteiinien sitoutumista mitataan kolmeen eri PP2A B alayksiköön B56γ, B56δ ja B56ε. Fosfoproteiini/α-endosulfiini perheen inhibiittoriproteiinien sitoutumisvoimakuutta tutkitaan kahden erilaisen fosforylaatiota matkivan mutaation avulla. Ensin B alayksikön proteiinit tuotettiin ja puhdistettiin, ja niiden proteiiniproteiini vuorovaikutuksia tutkittiin microscale thermophoresis menetelmällä. Tulokset osoittivat, että fosfoproteiini/α-endosulfiini perheen villityyppi proteiinit sitoutuivat kaikkiin tutkittuihin B56 alayksiköihin. CIP2A:n sitoutuminen oli vaihtelevaa. Fosforylaatiota matkivat mutaatiot lisäsivät sitoutumisvoimakkuutta cAMP-regulated phosphoprotein 19 kDa (ARPP19) ja cAMP-regulated phosphoprotein 16 kDa (ARPP16) kohdalla, mutta ei alfa-endosulfiinin (ENSA) kanssa.

TABLE OF CONTENTS

TERMS AND ABBREVIATIONS

TERMS

Holoenzyme	Enzyme in its active form that contains all its parts
Isoform	Similar protein groups that origin from the same gene that has undergone mutation
Kinase	Enzymes that transfers phosphates to substrates
Phosphatase	Enzymes that remove phosphatase from substrates
Phosphomimic	Protein that have their amino acid sequence changed to mimic phosphorylation
Subunit	Singular protein that assembles with other proteins to form protein complexes

ABBREVIATIONS

ARPP16	cAMP-regulated phosphoprotein 16 kDa
ARPP19	cAMP-regulated phosphoprotein 19 kDa
cdk1	Cyclin dependent kinase 1
CIP2A	Cancerous Inhibitor of PP2A
cycB	Cyclin B
ENSA	Alpha-endosulfine
GST	Glutathione S-transferase
Gwl	Greatwall
HEAT	Huntingtin, EF3, PP2A A subunit, and TOR1
MAST3	Microtubule-associated serine/threonine kinase 3
MASTL	Microtubule-associated serine/threonine kinase-like
MST	Microscale thermophoresis

PBS	Phosphate-buffered saline
PKA	Protein kinase A
PME-1	Methyl Esterase 1
PP2A	Protein phosphatase 2A
PPI	Protein-protein interaction
SEC	Size-exclusion chromatography
SET	Suvar 3-9/Enhancer of zeste/ Trithorax
TEV	Tobacco Etch Virus protease
TIP	Type 2A Interacting Protein
TRIC	Temperature related intensity change
WT	Wild type

1 INTRODUCTION

1.1 Kinases and phosphatases

Cells are under constant regulation by kinases and phosphatases. Kinases are enzymes that catalyse phosphate transfer reactions by phosphorylating their target. Phosphatases function other way around as phosphate group removers by dephosphorylating their targets. This regulation by kinases and phosphatases turn their target into active or inactive forms by either phosphorylating or dephosphorylating them depending which form is needed in cell at that time (Mumby and Walter 1993). Kinases can be divided into five group where the most common groups are, protein tyrosine kinases and protein serine/threonine kinases (Hunter 1991). Phosphatases consists of four families, phosphoprotein phosphatases, phosphoprotein metallophosphatases, phosphotyrosine phosphatases, and Asp-based protein phosphatases (Kerk et al. 2008). From these four families, phosphatases can function as protein tyrosine phosphatases and protein serine/threonine phosphatases. Phosphatases can form from monomers, dimers, or even bigger holoenzyme complexes. They are also known to include variety of different isomers between their different subunits. This function allows the same phosphatase to work in different tasks when it is equipped with different isoform (Seshacharyulu et al. 2013).

1.2 Protein phosphatase 2A

Protein phosphatase 2A (PP2A) is a major serine/threonine phosphatase that removes a phosphate group from its target protein. PP2A is a part of many different regulation processes that undergo inside cells. Its function mechanisms and subunit composition variation are still poorly understood, even though 1 % of all protein inside cells is PP2A (Cho and Xu 2007). PP2A interacts with various

signalling pathways, for instance pathways for regulation of the cell cycles, cell proliferation and neuronal signalling. Disturbance of these pathways can cause diseases like cancer, Alzheimer's disease, and depressive disorders (Musante et al. 2017). Therefore, it is important to further understand how PP2A is regulated in the cell.

The PP2A holoenzyme complex consists of three different subunits, A, B and C (Figure 1). The biggest subunit of this heterotrimeric enzyme is A subunit, and it functions as the scaffolding that keeps the whole structure together. It consists of 15 identical 40 amino acid HEAT repeats that are named after first recognized cytoplasmic proteins Huntingtin, Elongation factor 3, the PP2A A subunit, and yeast kinase TOR1. Each of the 40 HEAT repeats consists of two adjacent alpha helixes. The B subunit is the regulatory subunit and it is attached to A subunit at HEAT repeats 3-7. The C subunit is the catalytic subunit that is composed of globular α/β fold and it is attached to the A subunit at repeats 11-15 (Sangodkar et al. 2016).

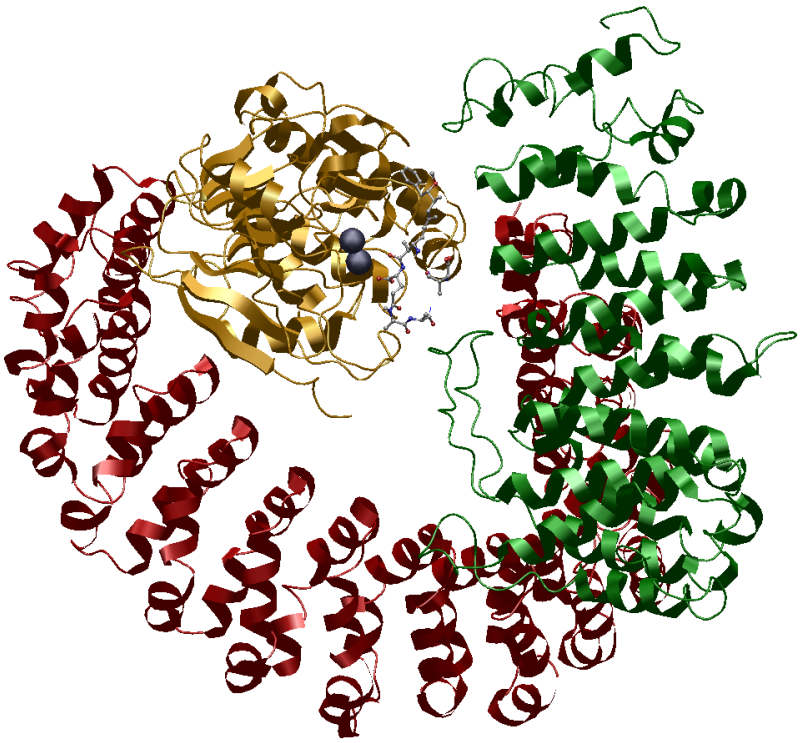

Figure 1. Structure of the PP2A holoenzyme. At the back side of the figure is the scaffolding A subunit (Red). At the front right is the regulatory B (B56) subunit (Green) and in the top middle is the catalytic C subunit (yellow). PDB: 2IAE

1.3 Isoforms of PP2A subunits

Protein isoforms are highly similar proteins that originate from same gene family that have overgone slight genetic changes. They usually have same biological roles their functions can still vary. PP2A is a heterotrimeric enzyme that has multiple isoforms in between its subunits. A and C subunits have only two isoforms α and β. B subunit has at least 23 different isoforms in different families (Haesen et al. 2014). These B subunits can be divided into four different families, B (also called B55), B′ (B56), B′′(PR72) and B′′′ (Stratin family), that differ from each other but contain similar isoforms within the family (Westermarck and Hahn 2008). From these, B55 and B56 subunit families are the most studied. B55 is 55 kDa subunit that interacts with a subunit HEAT at repeats 1-2 and 3-7 and is composed of seven WD terminating 40 amino acid repeats (Xu et al. 2008). Subunit B56 is 56

kDa subunit and it is composed of 8 HEAT-like repeats that interact with A subunit at HEAT repeats 2-8 and partly with C subunit (Sangodkar et al. 2016). When comparing two different B subunit families B55 and B56 to each other, it is seen that there are major structural differences between these families (Figure 2). B56 has 5 known isoforms B56α, B56β, B56γ, B56δ and B56ε. Similarity of these five isoforms was also studied in this research.

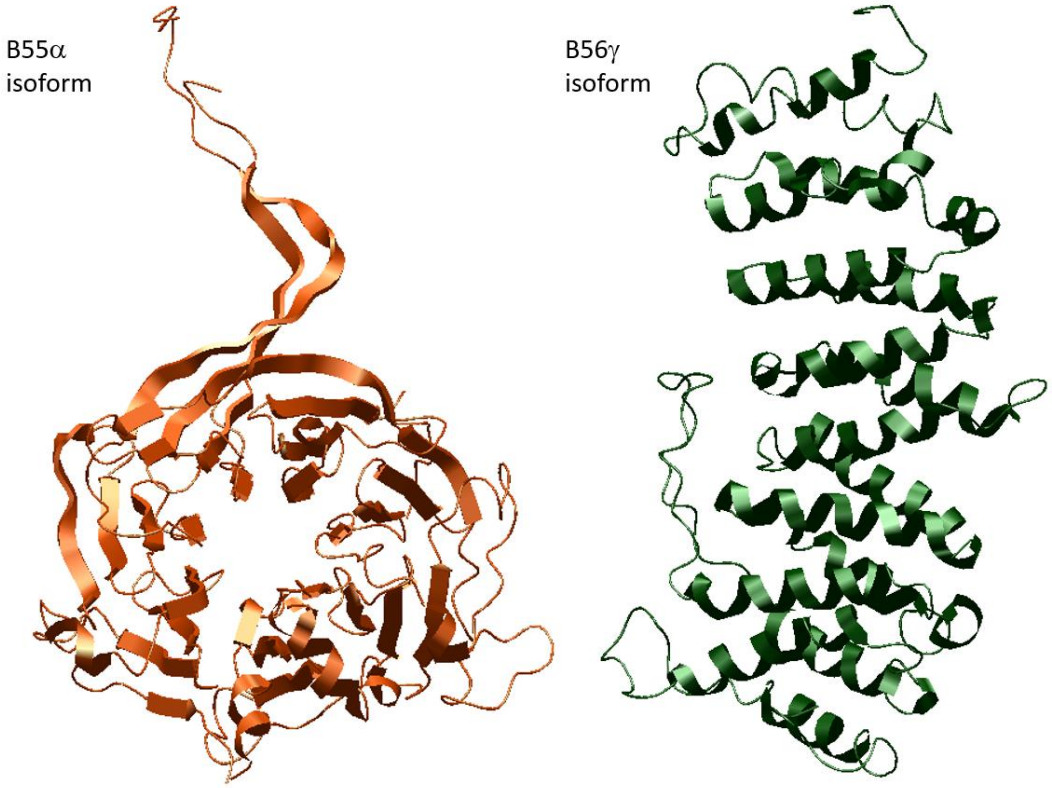

Figure 2. Protein structures of two different PP2A regulatory subunit families: B55 and B56. B55α on the left (Orange) and B56γ on right (Green). B55α from PDB: 3DW8 and B56γ from PDB: 2IAE.

1.4 Inhibitors of PP2A

As already said, diseases like cancer, Alzheimer's disease and depressive disorders can occur when signalling pathways of PP2A are disturbed by its inhibition (Musante et al. 2017). PP2A is a known tumour suppressor, and

inhibition of PP2A can remove its tumour suppression capabilities. As PP2A has central role in regulating many important cellular processes, it is important to study what causes PP2A suppression in cells. Many endogenous inhibitors have been discovered for PP2A. From these proteins like Cancerous Inhibitor of PP2A (CIP2A), proteins from cAMP regulated phosphoprotein/α-Endosulfin family, Suvar 3-9/Enhancer of zeste/ Trithorax (SET), Methyl Esterase 1 (PME-1) and Type 2A Interacting Protein (TIP) are all known to inhibit PP2A, which can lead to formation of cancer (Haesen et al. 2012). Currently, most of these PP2A inhibitors are still yet to be thoroughly studied and do not have solved dimensional structure.

1.4.1 ARPP19 and ARPP16

cAMP-regulated phosphoprotein 19 kDa (ARPP19) is an endogenous inhibitor protein for PP2A that belongs into cAMP regulated phosphoprotein/α-Endosulfin family (Labendera et al. 2015). It is regulated by cyclic adenosine monophosphate in order to regulate PP2A activity in cell. ARPP19 inhibits the PP2A B subunit so mitosis is started in cell cycle (Gharbi-Ayachi et al. 2010). However, over expression of ARPP19 can cause cancer and so it has become major target in the study of cancerous PP2A inhibitor proteins (Haesen et al. 2012, Jiang et al. 2016). cAMP-regulated phosphoprotein 16 kDa (ARPP16) is a splice variant of ARPP19, which is coded from the same gene but with an alternative starting point. ARPP19 has the same amino acid sequence than ARPP16 but it has additional 16 amino acids on its N-terminal end (Musante et al. 2017). ARPP16 is also known PP2A inhibitor, which is present in the brain and functions as brain neurotransmitter inhibitor for brain signals (Girault et al. 1990). Both ARPP19 and ARPP16 are intrinsically disordered proteins (Thapa et al. submitted).

1.4.2 ENSA

Alpha-endosulfine (ENSA) is also an endogenous inhibitor protein of PP2A which belongs to the same family as ARPP19 and ARPP16 (Horuichi et al. 1990,

Dulubova et al. 2001). Because ENSA is genetically related to ARPP19 and ARPP16, it shares high amino acid similarity and similar structure but has different N-terminal end (Heron et al. 1998). As they are in the same family, PP2A inhibition by ENSA functions similarly as ARPP19 inhibition (Gharbi-Ayachi et al. 2010). ENSA is a smaller protein with a molecular weight of 13.4 kDa. ENSA functions as a phosphatase inhibitor that inhibits normal functions of PP2A in human cells during mitosis. Phosphorylation of ENSA amino acid Ser-67 makes ENSA interact with PP2A B55 subunit (Heron et al. 1998). This interaction leads to PP2A inactivation in cells. ENSA is intrinsically disordered protein (Thapa et al. unpublished).

1.4.3 CIP2A

CIP2A is a protein that inhibits PP2A (Junttila et al. 2007). CIP2A inhibition of PP2A is particularly important in the regulation of protein kinase B. Protein kinase B, also known as Akt kinase, is a central cell growth regulator in human cells. One of the known targets of Akt is the transcription factor c-Myc, whose activation can lead to cancer and CIP2A activation can cause this cascade (Ding et al. 2018). The CIP2A dimer interacts with PP2A subunits B56α and B56γ (Wang et al. 2017). Molecular weight of the whole CIP2A is 102 kDa. CIP2A is a homodimer protein. From amino acids 1-560 is the 62.2 kDa core domain, 561-578 is the small 2.2 kDa intrinsically disordered region, 579-706 is a 14.3 kDa intrinsically disordered domain and from 706-905 another 23.4 kDa intrinsically disordered region (Wang et al. 2017, Thapa et al. unpublished). From all these parts, only the core domain from CIP2A structure has been solved (Figure 3).

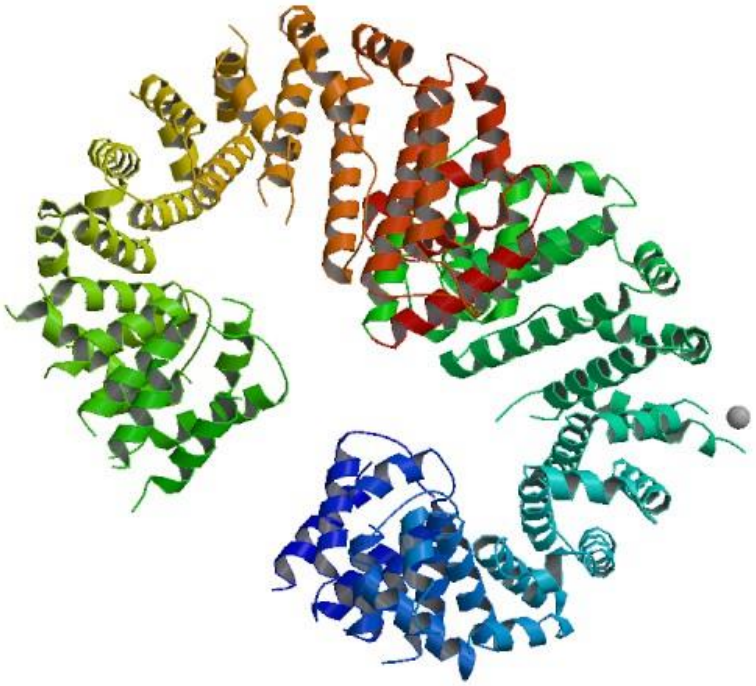

Figure 3. Structure of CIP2A protein containing amino acids 1-560. PDB: 5UFL

1.4.4 Other PP2A inhibitors

Protein SET is a one of the first known PP2A inhibitors. SET has two isoforms and both of them are potent inhibitors of PP2A on the side of being inhibitor to many other proteins as well (Beresford et al. 2001) PME-1 is an inhibitor and regulator for PP2A. The inhibition happens by demethylation of L309 of the PP2A C subunit (Ogris et al. 1999). TIP is ubiquitously expressed protein that inhibits and regulates PP2A. TIP inhibition is known to affect PP2A subunit C activity (McConnell et al. 2007). Potential therapeutic targeting for PP2A inhibitors have also been discovered but more information and further studies are still needed (O'Connor et al. 2018).

1.5 Phosphorylation of inhibitors

Inhibitor proteins are not always in their active form in cell. To activate them, different kinase proteins are needed as they can phosphorylate them into their active form. The three inhibitors studied here, that are active at the onset of the mitosis (ARPP19, ARPP16 and ENSA), are all activated by phosphorylation. This has been best studied with ARPP19. The main kinase responsible for ARPP19 activation is Greatwall (Gwl) kinase that phosphorylates ARPP19 at S62. This phosphorylation is part of a bigger signal chain to start the mitosis in cell (Mochida et al. 2014). In order to initiate mitosis, the cell needs to activate cyclin B (cycB) cyclin dependent kinase 1 (cdk1) complex, so it can inhibit the antimitotic PP2A. This complex activates Gwl that further phosphorylates ARPP19, which then inhibits PP2A (Gharbi-Ayachi et al. 2010). PP2A inhibition means that the substrates needed to start the M-phase are no longer dephosphorylated, so mitosis can begin. When cell cycle needs to move on to the interphase, cdk1 is inactivated by degeneration of cyclins so Gwl stops helping ARPP19 to inhibit PP2A and M-phase substrates are again dephosphorylated (Haccardo and Jessus 2011). This cycle can be seen in Figure 4. In this study, it is assumed that this similar activation can also happen with ARPP16 and ENSA, as they have similar properties than ARPP19.

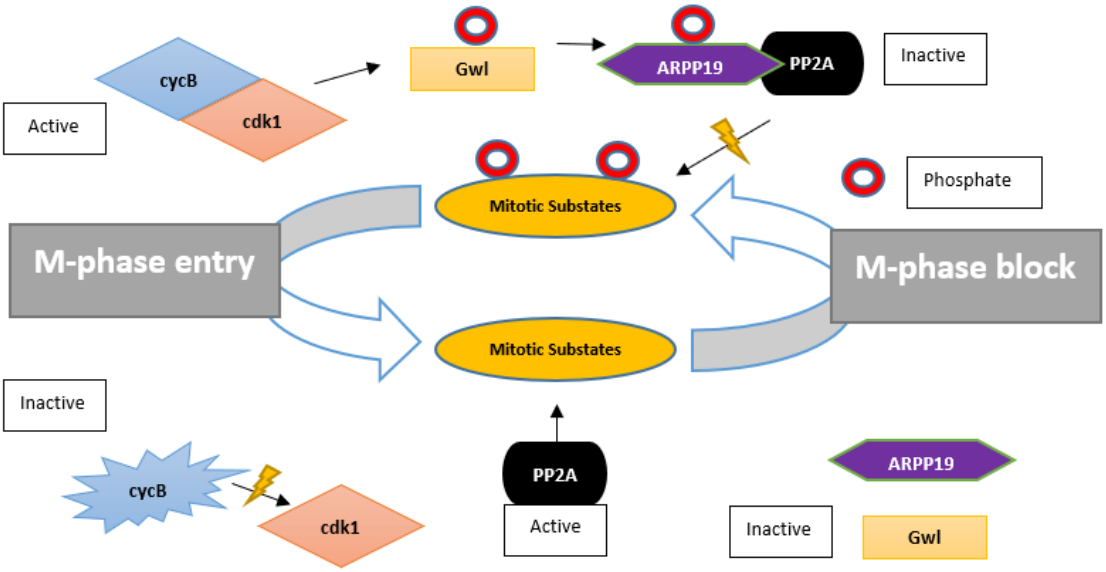

Figure 4. Inhibition of PP2A by ARPP19 to mediate cell cycle. In the top part of the figure, cycB is active and bound to cdk1. This activates Gwl by phosphorylating it which further phosphorylates ARPP19. In phosphorylated state ARPP19 inhibits PP2A, which stops dephosphorylation of mitotic substrates that functions as barrier in M-phase entry. Cell then passes to M-phase. In the lower part of the figure, when no longer needed cycB is inactivated by degeneration of cyclins and cannot start the signal cascade that leads to PP2A inactivation. This way PP2A can suppress mitotic substrates and cell is not able to enter M-phase.

Another kinase, microtubule-associated serine/threonine kinase 3 (MAST3), is known to phosphorylate ARPP16 at S46 that corresponds to S62 in ARPP19 (Andrade et al. 2017). Microtubule-associated serine/threonine kinase- like (MASTL) is a functionally same kinase as Gwl as it causes ARPP19 and ENSA phosphorylation activation (Voets and Wolthuis 2010). MASTL will cause phosphorylation of ENSA at S67 and ARPP19 at S62 (Kumm et al. 2020). In addition to S62 in ARPP19 (corresponding to S46 in ARPP16 and S67 in ENSA) also S104 of ARPP19 is frequently phosphorylated by protein kinase A (PKA), the cAMP regulated kinase (Kumm et al. 2020). This phosphorylation initially gave ARPPs their name (cAMP regulated phosphoprotein). However, it is unclear how

S104 phosphorylation at ARPP19 (or S88 in ARPP16 and S109 in ENSA) regulates its activity (Andrade et al. 2017). There is some evidence that *in vitro* ARPP16 S88 phosphorylation inhibits S46 phosphorylation by different kinases (Musante et al. 2017). These kinases, Gwl, MAST3, MASTL and PKA, combined seem to have two different serine sites that they phosphorylate in ARPP19, ARPP16 and ENSA that can be divided into N- and C-terminal serine. Also, it is clear that phosphorylation of these inhibitors is required in order for them to bind to PP2A. Importance of the effects of phosphorylation to PP2A inhibitor proteins, like CIP2A, can also be seen as they work together with phosphorylated PP2A substrates, like c-Myc oncogene, in order to cause cancer (Puustinen and Jäättelä 2014).

1.6 Phosphomimicking

The changes that kinases perform to their target proteins can be hard replicate outside of the cell. However, this phosphorylation can be at least partially mimicked by specific mutations to the protein. The site of the mutation is usually amino acids serine, threonine, and tyrosine that are target for phosphorylation by kinases in cell. These amino acids are changed to aspartic acid or glutamic acid, that are negatively charged and approximately the same size as the phosphate group would be. This mimics the phosphorylated wild type amino acid. The inhibitors, that are activated by phosphorylation, are similar to each other and share the two different serine sites where phosphorylation happens. For ARPP19 these sites are S62 and S104, for ARPP16 they are S46 and S88, and for ENSA they are S67 and S109 (Gharbi-Ayachi et al. 2010, Musante et al. 2017, Kumm et al. 2020). These sequences can be compared because all ARPP16, ARPP19 and ENSA belong to same phosphoprotein/α-endosulfin family (Figure 5) (Labendera et al. 2015). This phosphorylation is important because it allows these inhibitors to bind to PP2A. When changing these amino acids from serine to glutamic acid, it is possible to mimic phosphorylation of these serine sites. In this study, it is assumed that this phosphomimicking will increase the binding strength of the inhibitor

proteins to PP2A regulatory subunit B. This phosphomimicking mutation allows us to study the effects of phosphorylation in these inhibitor proteins, as they normally would be phosphorylated before the inhibition in cell.

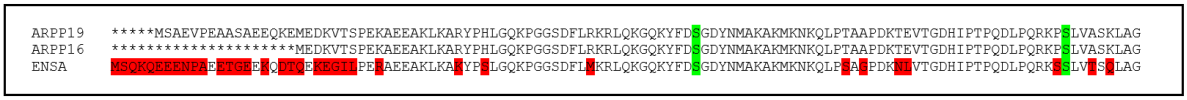

Figure 5. Amino acid sequence alignment of ARPP19, ARPP16 and ENSA. From N-terminal to C-terminal end. In green colour are similar serine amino acids that are mutated to glutamic acid: ARPP19 S62 and S104, ARPP16 S46 and S88, and ENSA S67 and S109. In red are sequence differences of ENSA.

1.7 Protein-Protein interaction

Protein-protein interactions (PPIs) are an essential part in countless biological processes. These processes occur because each protein is only capable of interacting with the proteins that it is supposed to interact with. PPIs form a basis for cellular structures and functions. In chemical sense PPIs are electrostatic forces, hydrogen bonds and hydrophobic effects between molecules. These interactions can happen between two or more proteins.

PPIs can be divided into different categories according how they interact with each other. One way is to sort them in obligate and nonobligate, where obligate proteins cannot exist without the other protein (Nooren and Thornton 2003). Another way is to study their binding where they can be divided into permanent and transient interactions (Perkins et al. 2010). Transient interaction can be further divided into strong and weak transient interactions. Permanent binding affinity is nM and weak transient binding affinity is μM.

As these interactions are important to cell, they are also important field to study. Many different methods have been used to do this and they all have their strengths and weaknesses, when comparing different aspects of the interaction (Miura 2018). These aspects can mean that the method can be used to study the

affinity, kinetics, or higher structure of the proteins. Proteins can also lose activity upon protein purification, so it is better to keep them as close as possible to their real environment (Jerabek-Willemsen et al. 2014).

1.8 Microscale thermophoresis

Microscale thermophoresis (MST) is a method that uses infrared lasers to measure molecular interaction between two biomolecules. This is done by measuring two different things, the changes in the movement of the molecule in temperature gradient (thermophoresis) and the temperature related intensity change (TRIC), at the same time. Binding-induced changes of two molecules affect the measurements of both thermophoresis and TRIC, which are then used to together to determine the overall MST signal. These can mean changes in many molecular properties, such as size, charge, hydration shell or conformation of the molecules (Seidel et al. 2013). In regular experiments one of the molecules has the fluorescent label and one is left un-labelled, to see changes in one molecule at a time. The fluorescent labels are used to detect and quantify the movement of the molecules. When proteins are measured in MST, ligand is usually left un-labelled and its concentration is varied when the concentration of the target protein is kept constant. MST is good method in detecting even slightest changes in molecular interaction and it can be used even in mixed solution that mimic real live conditions more precisely (Seidel et al. 2013).

Measurements in Monolith-series devices, in our case Monolith NT, are done in small capillaries that the MST machine individually heats and measures the fluorescence. During the measurement, the sample is heated locally with an infrared laser at 1480 nm wavelength to create a temperature gradient of 2-6 ^{o}C (Jerabek-Willemsen et al. 2014). This then gives the machine a signal from the label that is detected as an excitation light. When the target protein is measured with different concentrations of ligand in a dilution series, the data can be used to calculate binding affinity for the biomolecule pair. From each measurement of

binding, the MST machine defines a signal to noise ratio. Signal to noise ratio tells the quality of the measurement. It is calculated as the response amplitude of the signal divided by the mean of average standard deviation of all the points (NanoTemper 2011). This means if the signal to noise ratio is too low, the MST cannot detect binding.

1.9 The aim of the study

The aim of this research is to study binding mechanisms that PP2A inhibitory proteins use in the PP2A inhibition. This is done by performing binding experiment with MST to see if the different inhibitor proteins, ARPP19, ARPP16, ENSA and CIP2A, have difference in the interaction to the PP2A regulatory subunit B56 isoforms B56γ, B56δ, and B56ε. Another experiment is to see if the phosphomimicking mutants of ARPP16 (S46E or S88E), ARPP19 (S62E or S104E) and ENSA (S67E or S107E) increase their binding to the PP2A regulatory subunits B56 isoforms B56γ, B56δ, and B56ε. Also, the binding site of CIP2A is mapped to the PP2A regulatory subunit B56 isoforms B56γ, B56δ, and B56ε. This amount to 3 different PP2A B subunit isoforms and 11 different inhibitor proteins that combine into 33 different measurements. These measurements were done by measuring binding affinity between them with MST.

To study these interactions, the proteins first need to be expressed in bacteria and purified to acquire B56 protein that can be used in the MST measurements. Therefore, one aim was also to find working expression and purification protocols for these B56 isoforms. After this different B56 isoforms were measured in MST with each inhibitory protein to measure their binding affinity. Three adjacent measurements were done to each pair and the data was used to calculate binding affinity. Also, amino acid identity of B56 family isoforms B56α, B56β, B56γ, B56δ and B56ε was studied to see if they have differences that will affect their binding. Therefore, the binding of wild type inhibitor proteins, ARPP16, ARPP19, ENSA

and CIP2A, is compared to the PP2A regulatory subunit B56γ, B56δ, and B56ε to see if their binding to different isoforms differ.

The hypothesis is that the regulatory subunits, B56γ, B56δ, and B56ε, can be purified with similar protocols. Between different inhibitors, there are no differences in the interaction of the inhibitor proteins to the PP2A regulatory subunit isoforms B56γ, B56δ, and B56ε, because the all of the inhibitor proteins might bind to the same, conserved parts of these regulatory subunits. The phosphomimicking mutants of the N-terminal phosphorylation site increases the affinity, but those of the C-terminal site do not. This is because the different regulation kinase phosphorylates these sites. Also, the smaller domain of CIP2A interacts with PP2A regulatory subunits, because it is intrinsically unfolded as the other inhibitor proteins in these experiments that are known to bind to PP2A. The amino acid similarity will differ but all non-phosphorylated inhibitors will have similar low affinities when measured with the regulatory subunits or do not bind at all as they need phosphorylation in order to work.

2 MATERIALS AND METHODS

2.1 Materials

The regulatory B subunit B56 isoforms of PP2A (B56γ (UniProt accession number: Q13362-1), B56δ (Q14738-1) and B56ε (Q16537-1)) have been previously cloned into plasmid pGTvl 1-SGC by research group of Ulla Pentikäinen. These plasmids were used in transformation. This plasmid contains the gene sequence for each protein accompanied with gene for ampicillin resistance. The plasmid gene is also modified to expresses B56 isoforms attached to glutathione S-transferase (GST) with Tobacco Etch Virus (TEV) protease cut site in between. Already purified

inhibitory proteins were also obtained from the research group of Ulla Pentikäinen, so only B56 isoforms were expressed and purified in this research.

2.2 Methods

2.2.1 Expression

First step of protein production is to transform wanted plasmid to bacterial cell and induce them to express it. This was done by transforming 1 µl of each pGEX_B56 isoform plasmid (~ 200 ng/µl) to individual 50 µl of $CaCl_2$-competent *E. coli* BL21 DE3 GOLD cells. Transformation was done by heat shock and 450 µl of super optimal broth was added to it. These plasmids contain antibiotic resistance to ampicillin, so they were plated on lysogen broth agar plates that contain 100 µg/ml of ampicillin. Plates were incubated over night at 37 °C. One of the grown colonies was used to start pre-culture in terrific broth medium that had 100 µg/ml of ampicillin and 2 % glucose. After 16 h the culture was expanded into 1 l of same medium from 20 ml pre-culture. Cells were inoculated in shaker at 37 °C until OD_{600} was measured to be 0.6 (Ultrospec 2000 UV/Visible spectrometer, Pharmacia Biotech). After this the culture was cooled to 18 °C and induced with 0.4 mM of Isopropyl β- d-1-thiogalactopyranoside. Cells were then induced over night at 18 °C. Next day the cells were harvested by centrifugation at 6000 x g and 4 °C for 20 min. Pellet was washed by resuspending it to 1 x phosphate-buffered saline (PBS) and centrifuged again at 4000 x g and 4 °C for 30 min. Pellets were resuspended again into PBS and stored in -80 °C.

2.2.2 Purification

First the thawed pellet was lysed with sonicator (Bandelin electronic, Sonoplus HD 4100, UW 100, TS113) using 40 % of amplitude with 1 s sonication and 1 s rest for 1 min then repeated 4 times. Then the sample was left at 4 °C under slow rotation for 30 min. Sample was then centrifuged at 15 000 x g for 30 min at 4 °C. Then supernatant was poured on pre-equilibrated glutathione agarose (Protino

Glutathione Agarose 4B, Machery-Nagel, lot# 18121001), 6 ml for 1 l expression, in a column. Proteins were expressed as GST fusion protein which binds to glutathione agarose. Protein was left to bind to the resin for 2 h at 4 °C under slow rotation. After rotation, the unbound proteins were flown out slowly by gravity and the resin was washed with wash buffer (50 mM NaH_2PO_4, 150 mM KCl, 0.05 % CHAPS, 2 mM DTT). All the buffers have specific pH values, pH 6.8 for B56δ and pH 7.5 for B56γ and B56ε, according to their different protein pI values, B56γ pI 6.4, B56δ pI 8.2 and B56ε pI 6.5. Column was washed until A_{280} of the drops were measured under 0.1 ng/µl by NanoDrop (ND-1000, Thermo scientific). Then GST was cleaved off in the column by adding 500 ml of TEV (A_{280} = 1.08) with 4.5 ml of buffer and incubated over night at 4 °C under slow rotation. The TEV protease cleavage extended the constructs in the N-terminal by one amino acid residue, S.

Protein was collected using gravity flow and remaining protein was eluted with buffer. Fractions that have A_{280} higher than 0.1 ng/µl were pooled together. B56 proteins are easily aggregated when concentrated with centrifugal concentrators (Amicon Ultra 30 K, Millipore, lot# UFC903024), so only slight concentration is possible before size exclusion chromatography (SEC). SEC is run with ÄKTA prime plus (GE healthcare) and HiLoad 16/60 superdex 200 pg column (GE healthcare). SEC run was made with 1 ml/min flow speed and 2 ml fractions. Buffer used in SEC was 50 mM NaH_2PO_4, 75 mM KCl, 0.03 % CHAPS, 2 mM DTT. Fractions that had B56 were pooled together and concentrated with centrifugal concentrator. Final product was divided and stored in -80 °C to be used MST experiments.

2.2.3 MST experiments

In order to measure protein interaction with MST, one of the proteins needs to be labelled. In these experiments B56 isoforms were labelled with NT protein labelling kit red NHS according to instruction (Monolith NT-647-NHS, #MO-L001, NanoTemper) and inhibitor proteins were left unlabelled. Samples were measured

with Monolith NT. Automated Microscale Thermophoresis machine (NanoTemper technologies) with Monolith NT Automated Premium capillary chips (MO-AK005, NanoTemper) to determine dissociation constant K_d to each pair. B56 isoforms had concentration of 20 μM diluted in SEC buffer with 0.1 % Tween 20 through whole measurement. For the inhibitors, the upper and lower limit for their binding was determined and then dilution series 1:2 was performed with three repeated measurements. These triplicate experiments were done from each isoform and inhibitor protein pair. Results were analysed and made into graphs with GraphPad Prism 8 (version 8.1.2) using equation

$$Y = (Y0 - NS)^{(-K\,X)} + NS$$

where Y is total binding normalized (‰), $Y0$ binding at time zero normalized (‰), NS slope of nonspecific binding (‰/M), K rate constant (1/M) and X is ligand concentration (M). K_d measurement were done using single site total binding model in GraphPad Prism 8 (version 8.1.2) from the equation

$$Y = \frac{Bmax\ X}{(Kd + X)NS\ X + BG}$$

where Y is total binding normalized (‰), $Bmax$ maximum specific binding, X ligand concentration (M), NS slope of nonspecific binding (‰/M) and BG is background signal normalized (‰).

2.3 Similarity between B56 isoforms

All five B56 family isoforms, B56α, B56β, B56γ, B56δ and B56ε, were studied for amino acid similarity. Amino acid sequences from UniProtKB was aligned with the UniProtKB alignment program. UniProt codes 2A5A_HUMAN (B56α), 2A5B_HUMAN (B56β), 2A5G_HUMAN (B56γ), 2A5D_HUMAN (B56δ) and 2A5E_HUMAN (B56ε) were aligned together to show general similarity and individually compared to each other to determine identity.

3 RESULTS

3.1 Expression and purification of B56 proteins

This expression and purification protocol proved to work. Final concentrations were for B56γ 5.7 mg/µl, for B56δ 0.84 mg/µl and for B56ε 2.2 mg/µl. For each isoform 1 l expression yielded for B56γ 10 g, for B56δ 1g and for B56ε 4g of purified protein. The chromatogram from SEC and PAGE gel show that the final product, in this case B56γ, is also relatively pure (Figure 6). The same expression and purification protocol work for all three of these isoforms, except the buffer pH needs to be changed according the isoform pI.

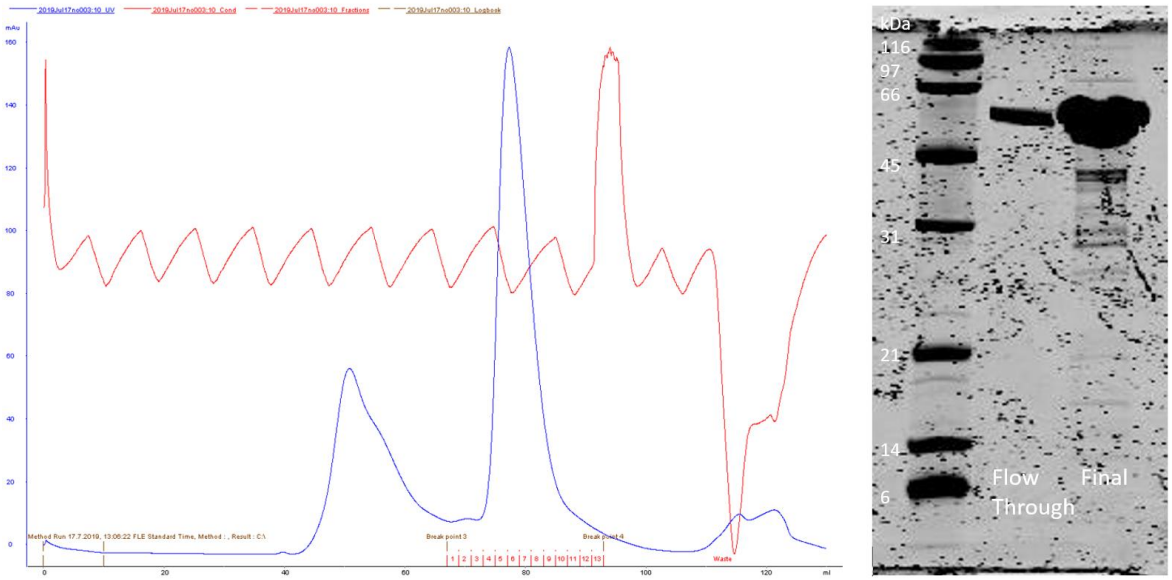

Figure 6. Chromatogram and PAGE gel from B56γ purification. At the left the blue line shows the SEC UV of 280 nm, where the B56 isoforms are seen after 90 ml as the highest peak. The red line shows conductivity. At the right is PAGE gel from the final concentrated sample showing the purity of B56γ.

3.2 Binding experiments

All different PP2A regulatory B subunit isoforms and inhibitory protein pairs were measured with MST. One B56 isoform is presented with each inhibitor and its phosphomimicking mutants, this makes total of 11 different inhibitors. Some of the measured PP2A B subunit that were tested did not show binding at all. Graphs of binding experiments of different B56 isoforms with each inhibitor and its possible mutants or parts are shown in figures below. They are presented in x-axis as 1:2 dilution series of ligand concentrations compared to the normalized fluorescence from 0 to 1 of the unbound and bound state of the B56 isoform and inhibitor concentration is presented in y-axis. The Kd value from each successful binding affinity measurement was also calculated. Also, the amino acid similarity of PP2A regulatory subunit B56 isoforms was compared to each other and binding of each wild type inhibitor to B56γ, B56δ and B56ε was compared.

3.3 B56γ with inhibitors

Interactions of PP2A subunit B56γ was measured with ARPP19wt, ARPP19S62E, ARPP19S104E, ARPP16wt, ARPP16S46E, ARPP16S88E, ENSAwt, ENSAS67E, ENSAS109E, CIP2A 1-560 and CIP2A 579-706 (Figure 7).

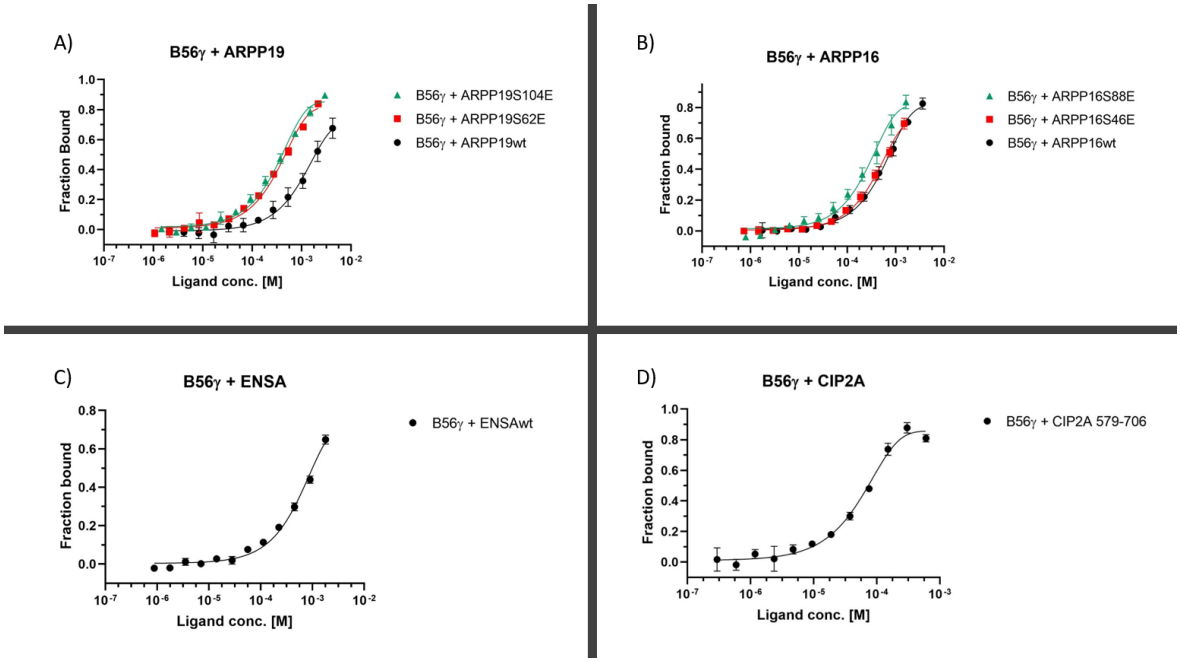

Figure 7. B56γ binding affinity curves with measured inhibitors proteins studied. Section A has B56γ measured with ARPP19wt (black), ARPP19S62E (red) and ARPP19S104E (green). Section B has B56γ measured with ARPP16wt (black), ARPP16S46E (red) and ARPP16S88E (green). Section C has B56γ measured with ENSAwt. Phosphomimicking mutants ENSAS67E and ENSAS109E did not bind into B56γ. Section D has B56γ measured with CIP2A 579-706. CIP2A 1-560 did not bind.

The interaction of B56γ was measured with ARPP19wt and its phosphomimicking mutants ARPP19S62E and ARPP19S104E. Binding experiment (Figure 7, A) shows that ARPP19wt had significantly weaker binding affinity than the phosphomimicking mutants. Even though the binding affinity of the ARPP19S62E and ARPP19S104E were almost the same ARPP19S104E had a little bit stronger binding.

Similarly, binding of B56γ with ARPP16wt and its phosphomimicking mutants ARPP16S46E and ARPP16S88E was measured. Binding experiment (Figure 7, B) showed that ARPP16wt had the weakest binding affinity from ARPP16 variants and the binding affinity of ARPP16S46E was second weakest, but almost the same as ARPP16wt. ARPP16S88E had strongest binding affinity that separates clearly from the two others.

Then, B56γ's interaction with ENSAwt and its phosphomimicking mutants ENSAS67E and ENSAS109E was measured. When measuring the MST, neither of the phosphomimicking mutants showed big enough signal to noise ratio to detect binding. On the other hand, binding affinity was able to be determined from ENSAwt even though it did not fully saturate from the top (Figure 7, C).

Also, the interaction of B56γ CIP2A 1-560 and CIP2A 579-706. When measuring with MST, CIP2A 1-560 did not have big enough signal to noise ratio to show binding. Binding affinity was still able to be measured with CIP2A 579-709 (Figure 7, D).

3.4 B56δ with inhibitors

The interaction of PP2A B56δ subunit with ARPP19wt, ARPP19S62E, ARPP19S104E, ARPP16wt, ARPP16S46E, ARPP16S88E, ENSAwt, ENSAS67E, ENSAS109E, CIP2A 1-560 and CIP2A 579-706 were measured in a similar way as to B56γ (Figure 8).

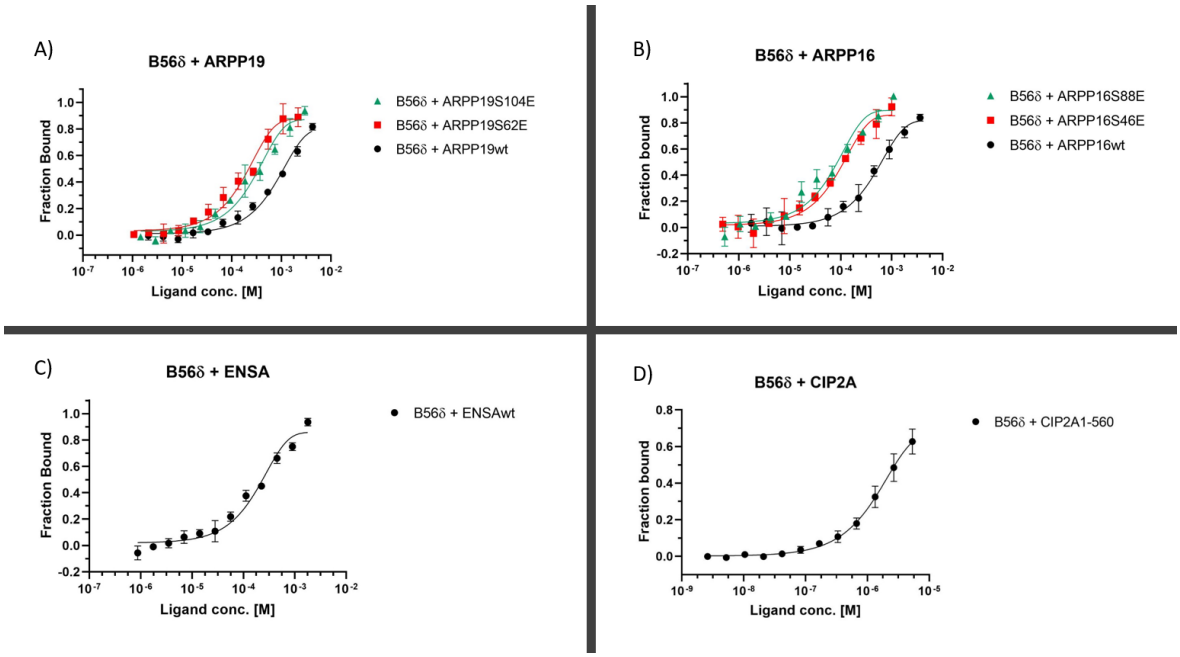

Figure 8. B56δ binding affinity curves with all inhibitor proteins studied. Section A has B56δ measured with ARPP19wt (black), ARPP19S62E (red) and ARPP19S104E (green). Section B has B56δ measured with ARPP16wt (black), ARPP16S46E (red) and ARPP16S88E (green). Section C has B56δ measured with ENSAwt. Phosphomimicking mutants ENSAS67E and ENSAS109E did not bind into B56δ. Section D has B56δ measured with CIP2A 1-560. CIP2A 579-706 did not bind.

Binding experiment of B56δ with ARPP19wt and its phosphomimicking mutants ARPP19S62E and ARPP19S104E (Figure 8, A) showed that ARPP19wt had the weakest binding affinity from these three inhibitory proteins. The phosphomimicking mutants ARPP19S62E and ARPP19S104E had stronger binding and from those two the higher binding affinity was with ARPP19S104E. In the graph the curve for ARPP19S104 has not reached its upper saturation so the strength of the binding is estimated to be at least this high.

Then, B56δ's interaction with ARPP16wt and phosphomimicking mutants ARPP16S46E and ARPP16S88E was measured. Binding experiment (Figure 8, B) showed that ARPP16wt had the weakest binding affinity. ARPP16S46E and ARPP16S88E had clearly higher binding affinity than ARPP16wt and ARPP16S88E had the highest binding affinity of the two.

Also, B56δ's interaction with ENSAwt and phosphomimicking mutants ENSAS67E and ENSAS109E was measured. When measuring with MST, either of the phosphomimicking mutants did not have big enough signal to noise ratio to show binding. Measurements with ENSAwt showed binding (Figure 8, C) and binding affinity was determined.

Measurements of B56δ interaction with CIP2A 1-560 and CIP2A 579-706 was then conducted. When measuring with MST, CIP2A 579-706 did not have big enough signal to noise ratio to show binding. Binding affinity was still able to be measured for CIP2A 1-560 even though it did not fully reach saturation (Figure 8, D).

3.5 B56ε with inhibitors

The interaction of PP2A subunit B56ε was measured with ARPP19wt, ARPP19S62E, ARPP19S104E, ARPP16wt, ARPP16S46E, ARPP16S88E, ENSAwt, ENSAS67E, ENSAS109E, CIP2A 1-560 and CIP2A 579-706 in a similar way to that of the above-mentioned B56 isoforms (Figure 9).

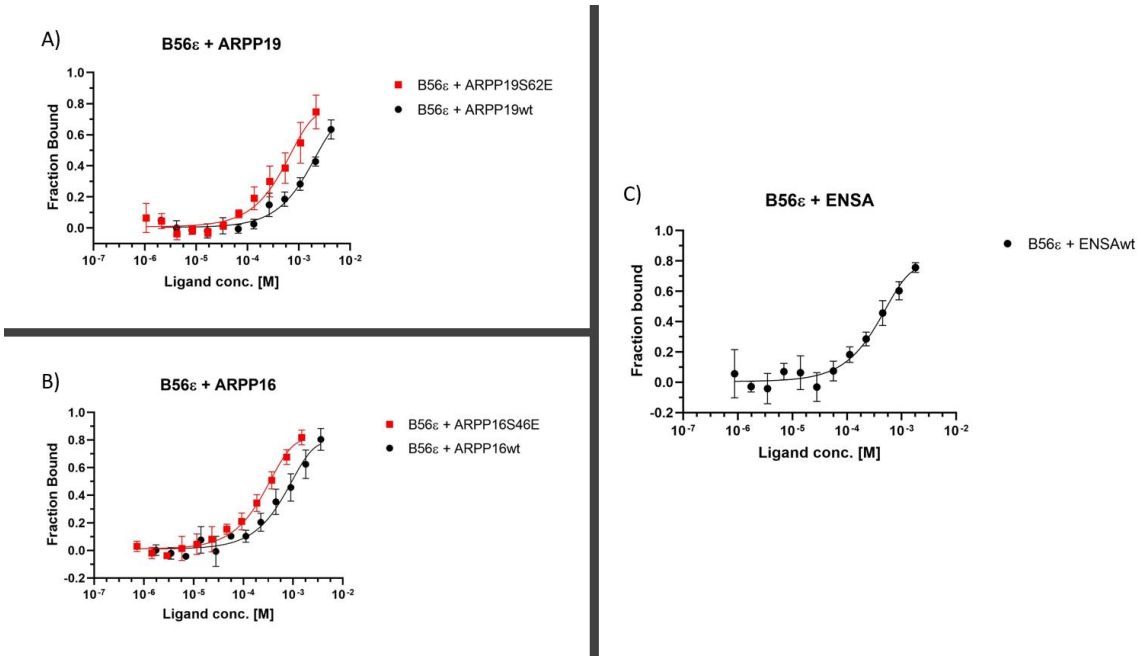

Figure 9. B56ε binding affinity curves with all inhibitor proteins studied. Section A has B56ε measured with ARPP19wt (black) and ARPP19S62E (red). ARPP19S104E did not bind. Section B has B56ε measured with ARPP16wt (black) and ARPP16S46E (red). ARPP16S88E did not bind. Section C has B56ε measured with ENSAwt. Phosphomimicking mutants ENSAS67E and ENSAS109E did not bind into B56ε. CIP2A 1-560 and CIP2A 579-706 were also measured but they did not bind into B56ε.

The interactions of B56ε was measured with ARPP19wt and its phosphomimicking mutants ARPP19S62E and ARPP19S104E. ARPP19S104E did not have big enough signal to noise ratio to conclude binding in MST experiments. Binding experiment (Figure 9, A) showed that ARPP19wt has weaker binding affinity to B56ε than ARPP19S62E. Also, either of these binding affinity curves did not reach full saturation.

Similarly, binding of B56ε was measured with ARPP16wt and phosphomimicking mutants ARPP16S46E and ARPP16S88E. In MST measurement, ARPP16S88E did not have big enough Signal to noise ratio so binding could not be conducted. Binding experiment (Figure 9, B) showed that ARPP16wt had the weaker binding affinity than ARPP16S46E.

Also, binding of B56ε was measured with ENSAwt and phosphomimicking mutants ENSAS67E and ENSAS109E. When measuring the proteins with MST, either of the phosphomimicking mutants did not have big enough signal to noise ratio to show binding. Measurements with ENSAwt showed binding (Figure 9, C) and binding affinity was determined.

B56δ interaction was also measured with CIP2A 1-560 and CIP2A 579-706. When measuring each part of CIP2A with MST, the measurements did not show big enough signal to noise ratio to conclude binding for either of the CIP2A domains.

3.6 Kd values

All the results from binding affinity are also marked in numerical form (Table 1). Here all values are presented as μM concentrations. The binding affinity concentrations are the values where half of the inhibitor protein is in bound state. These numbers represent the highest binding affinity because in all cases the upper saturation was not fully reached with the substrate concentrations that we had in our use. Overall, the Kd values of all the pairs were around 1-1000 μM. Binding affinity between B56 isoforms and ARPP19wt, compared to its phosphomimicking mutants, the phosphomimicking mutants had binding two or three times stronger in all the isoforms. Binding between B56 isoforms and ARPP16wt, compared to its phosphomimicking mutants, showed similar results as ARPP19. Exception was B56δ, where the phosphomimicking mutants showed 10-20 times stronger binding than ARPP16wt. ENSAwt compared to ARPP19wt and ARPP16wt had two to four times stronger binding affinity in all isoforms, except B56ε where the binding was similar. CIP2A 1-560 measured with B56δ, had many times stronger binding than any of the other pair but CIP2A 579-706 measured with B56γ had similar binding affinity as the strongest binding affinities of the other wild type proteins.

Table 1. Binding affinity between B56 isoforms and inhibitor proteins. Binding affinity for each isoform B56γ, B56δ and B56ε are presented with all inhibitors, their phosphomimicking mutants and different domains. These numbers are in µM concentration. Parts of the table that do not have numerical value did not show binding in the MST test as signal to noice ratio was too low to conclude their binding.

Binding affinity of B56 isoforms (µM)				
ARPP19		B56γ	B56δ	B56ε
	WT	<1200	<440	<810
	S62E	<340	<220	<330
	S104E	<320	<160	-
ARPP16		B56γ	B56δ	B56ε
	WT	<720	<740	<450
	S46E	<450	<85	<260
	S88E	<190	<34	-
ENSA		B56γ	B56δ	B56ε
	WT	<250	<120	<590
	S67E	-	-	-
	S109E	-	-	-
CIP2A		B56γ	B56δ	B56ε
	1-560	-	<3.4	-
	579-706	<190	-	-

3.7 Amino acid identity of B56 isoforms

Results studying amino acid identity between PP2A regulatory B subunit B56 family isoforms, B56α, B56β, B56γ, B56δ and B56ε, showed that all the isoforms have major differences between each other. Most similar parts of the isoforms, when comparing amino acids sequence, are in the middle of the sequence and

both N- and C-terminal ends show most of the varying parts (Appendix 1.) Amino acid sequences of each B56 isoforms are also compared to each other (Table. 2). Highest amino acid identity was between B56α, B56β and B56ε. Also, B56γ and B56δ shared similarity.

Table 2. Amino acid identity between B56 isoforms. Percentage of each B56 isoform pair amino acid sequence similarity is calculated and showed in accordance to each other.

%	B56α	B56β	B56γ	B56δ	B56ε
B56α	100	67.47	53.92	50.75	74.49
B56β		100	52.41	51.24	67.40
B56γ			100	67.28	55.60
B56δ				100	51.82
B56ε					100

3.8 Comparison of B56 isoforms

Inhibitor binding between different B56 isoforms were also compared (Figure 10). This was done with wild type of ARPP19, ARPP16 and ENSA because they were only inhibitors that had binding affinity with all B56 isoforms.

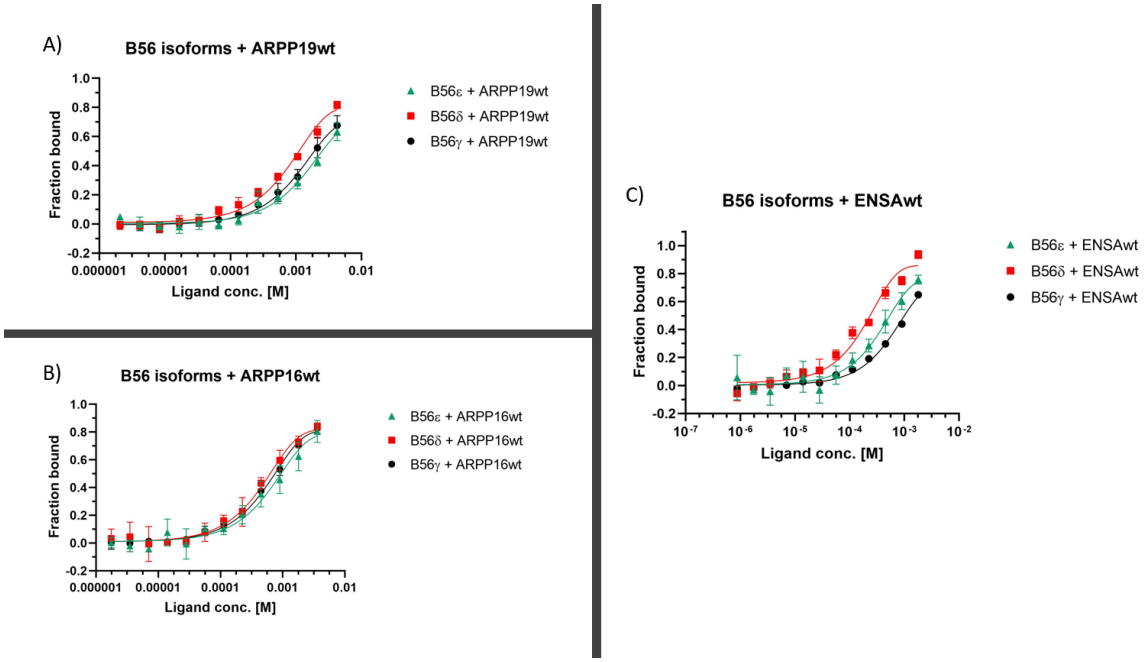

Figure 10. Binding curves comparing B56 isoforms and wild type inhibitor proteins. Section A has B56γ (black), B56δ (red) and B56ε (green) measured with ARPP19wt. Section B has B56γ (black), B56δ (red) and B56ε (green) measured with ARPP16wt. Section C has B56γ (black), B56δ (red) and B56ε (green) measured with ENSAwt.

B56 isoform comparison for ARPP19wt (Figure 10, A), showed that B56δ has the strongest binding with it. B56γ and B56ε similar but weaker binding. When comparing data from all binding affinity tests with ARPP16wt (Figure 10, B), all B56 isoforms had similar binding. B56ε had a little stronger binding than the other two isoforms. Measurements done between B56 isoforms and ENSAwt (Figure 10, C) showed that B56δ has the strongest binding with it. Next was B56γ but with high error value B56ε also showed similar binding. Position of these curves and their numerical binding value from Table 1 have differences because the binding affinity of some of the curves has not reached its upper saturation limit. CIP2A fragments did not bind to all B56 isoforms so their binding could not be compared.

4 DISCUSSION

4.1 Expression and Purification

This expression and purification protocol proved to work as the final product was concentrated and pure enough to use in further studies. Even though there was lots of protein, the final concentration was still a bit low. This was because the concentration process of B56 isoform proteins was difficult. The B56 isoform proteins aggregate easily and is lost during the process. One way to get the highest concentration possible is to take the highest peak fraction straight from the SEC run and use it without pooling and concentrating it with the other fractions. Other lines, than B56, seen in PAGE gel (Figure 6.) were consistent with all the isoforms but are in so low concentration that they do not matter when using the B56 isoforms in further tests.

4.2 Binding experiments

Results for each binding experiment showed how complex and divergent individual protein-protein interactions are. When comparing overall inhibitor binding to all B56 isoforms, there are some differences between them. CIP2A domains have the strongest binding when they show binding. After that ENSA seems to have second strongest binding, although its phosphomimicking mutants did not bind to any of these B56 isoforms. ARPP19 and ARPP16 had the weakest binding from this group of inhibitors, but they bound equally strong comparing to each other. In the larger scale there are no differences in the interaction of the inhibitors to the regulatory subunits, because the all the inhibitors are intrinsically disordered (Thapa et al. unpublished). Only exception is CIP2A 1-560, which is not intrinsically disordered and has notably higher binding affinity.

4.2.1 ARPP19

In the measurements with ARPP19 and its phosphomimicking mutants, all B56 isoforms showed binding except the B56ε with ARPP19S104E. Clearly, the weakest binding was seen between ARPP19wt and B56γ. Phosphomimicking mutants ARPP19S62E and ARPP19S104E showed stronger binding in all successful binding experiments. Strongest binding was when ARPP19S104E and B56δ was measured together and it could be considered to also have overall strongest binding from the three options. Binding of these inhibitor proteins to B56α have shown similar results as B56δ but ARPP19S104E did not bind to B56α any stronger than ARPP19wt (Thapa et al. submitted).

4.2.2 ARPP16

When looking all B56 isoforms measured with ARPP16 and its phosphomimicking mutants, only B56ε and ARPP16S88E pair did not show binding, all other binding affinities could be concluded. Similarly, like with ARPP19, the ARPP16wt showed weaker binding with B56 isoforms than phosphomimicking mutants. Both phosphomimicking mutants bound stronger to the B56 isoforms, with ARPP16S88E showing the strongest overall binding with B56δ. Binding of ARPP16wt to B56α has given even weaker binding affinity than to our measured isoforms but phosphomimic mutants show similar binding (Thapa et al. submitted).

4.2.3 ENSA

Binding affinity could not be calculated to ENSA phosphomimicking mutants. Weak binding was observed but signal to noise ratio was high enough to conclude binding event. ENSAwt and all B56 isoforms on the other hand had binding, with B56δ it was strongest and with B56ε weakest. ENSAwt binds to B56α stronger than to these isoforms, and these phosphomimicking mutants have shown binding to B56α (Thapa et al. submitted).

4.2.4 CIP2A

Binding experiments were hard to measure with CIP2A constructs and B56 isoforms. The full length CIP2A cannot be used in these experiments because there is no way to purify it from E. coli or even insect cells currently (Wang et al. 2017). In our experiment only CIP2A 1-560 and CIP2A 579-706 are used to study binding because they can be purified. We were only able to calculate the binding affinity between CIP2A 1-560 and B56δ, and CIP2A 579-706 and B56γ. For the rest of the measurements signal to noise was too low to conclude any kind of binding. Binding between CIP2A 1-560 and B56δ had the strongest binding between any of the other pairs, only couple μM. From these two measurements that gave numerical binding affinity, CIP2A 579-706 seems to bind weaker. CIP2A 1-560 is a normal structural domain, whereas CIP2A 579-706 is intrinsically disordered part (Wang et al. 2017, Thapa et al. unpublished). The more stable structure of the CIP2A domains seems to lead to stronger binding.

4.3 Phosphomimicking mutants

When comparing binding between the wild type proteins and the phosphomimicking mutants it seems that ARPP19 and ARPP16 phosphomimicking mutants show better binding with all B56 isoforms, but ENSA phosphomimicking mutants did not. In most of the cases binding force has doubled or tripled when using phosphomimicking mutants. Between ARPP16wt and its phosphomimicking mutants with B56δ the strength of the binding was over ten times stronger. Exception is the ARPP19S104E and ARPP16S88E with B56ε that did not bind at all. Reason why ENSA phosphomimicking mutants did not show binding was probably because their interaction to these B56 isoforms was too weak. Also, ENSA might be more suitable inhibitor only for PP2A containing other regulatory subunits. When comparing these findings to ARPP19, ARPP16 and ENSA activation by phosphorylation, it can be said that the phosphomimicking mutation can help with the binding for ARPP19 and ARPP16,

but not for ENSA (Gharbi-Ayachi et al. 2010, Musante et al. 2017). One thing that can also be seen from the results is that with ARPP19 and ARPP16 always the more C-terminal phosphomimicking mutant had stronger binding to B56γ and B56δ. This might mean that this C-terminal serine is more important in phosphorylation than the N-terminal. With B56ε the more C-terminal phosphomimicking mutants on the other hand always failed. This might suggest that there is a structural difference in B56ε isoform that could block the inhibition.

4.4 Comparing isoforms

PP2A regulatory B subunit B56 family isoforms B56α, B56β, B56γ, B56δ and B56ε have notable differences in their amino acid sequences. B56α, B56β, and B56ε have more similar amino acid identity between each other than with B56γ and B56δ. B56γ and B56δ on the other hand form a pair that have more similar amino acid identity. Between all the isoforms the amino acid identity is only 50-75 % which means that all the isoforms contain regions that do not match with each other. This explains how the binding can differ so much between these isoforms. The amino acid identity similarity of B56γ and B56δ, compared to B56ε, does not show in the binding affinity measurements.

When comparing each B56 isoform, in the way the ARPP19 and ARPP16 inhibitors bind to them, there are differences. Generally, the B56δ isoform was more sensitive to binding when measuring with these inhibitors. Same way, the B56γ isoform had generally the weakest binding affinity from this group. B56ε on the other hand had binding affinity value between the two other isoforms, but B56ε was the only one to have inhibitors ARPP19S104E and ARPP16S88E not bind to it. With ENSA B56δ had still the strongest binding with B56ε having the weakest and B56γ being in the middle of them. Poor binding of B56ε still continued with CIP2A parts but the whole B56 subunit did not have predictable pattern of binding with CIP2A parts but only couple different successful measurements.

Prior to this experiment, these inhibitor proteins have already been known to bind to some PP2A subunits. There has been evidence that CIP2A 1-560 dimer interacts with PP2A subunits B56 (Wang et al. 2017). These results say that CIP2A 1-560 binds to B56α and B56γ isoforms. These results could not be repeated in our experiments with B56γ. ARPP19 is known to inhibit PP2A B subunit so mitosis can be started (Labendera et al. 2015). This is also seen in these experiments with all B56γ, B56δ and B56ε isoforms. When comparing these binding affinity results of PP2A regulatory B subunit B56 to the scaffolding A subunit, binding ARPP19 and ARPP16 to A subunit is stronger (Thapa et al. submitted). In these experiments the binding of ARPP19 and ARPP16 show binding affinity of 1-10 μM. This shows that the inhibitor protein binding to the whole heterotrimeric holoenzyme might have different results than individual subunit testing.

MAST3 kinase phosphorylated ARPP16 is known to inhibit B55α and B56γ, as it phosphorylates the more N-terminal S46 amino acid (Andrade et al. 2017). Phosphomimicking ARPP16S46E binding to B56γ shows this binding as well but the more C-terminal ARPP16S88E shows stronger binding than the N-terminal phosphomimicking mutation. Studies made with PKA phosphorylated C-terminal ARPP19 and ENSA show that with this activation these inhibitor proteins will bind to B56δ (Kumm et al. 2020). This was only seen in our tests with ARPP19 as phosphomimicking mutants did not bind to ENSA. Reason for this might be that our inhibitor proteins are only phosphomimicking proteins and the real phosphorylation has still slightly different properties than phosphomimicking these proteins. Phosphorylation of S67 of ENSA has shown binding to B55 subunit (Heron et al. 1998). This might mean that phosphorylated ENSA is interacting more with the B55 family than B56 family and therefore these phosphomimicking mutations did not show binding in this experiment.

4.5 Things to be taken in account for

In all graphs, the lower plateau of saturation can be clearly seen. Most if not all the graphs on the other hand do not have clear plateau at higher concentrations or it is not reached at all. This means that the calculations for the Kd of these protein-inhibitor pairs might not be totally reliable but a value to estimate the binding can still be presented. The saturation level was not reached because the concentration in which the inhibitor proteins were measured could not be concentrated more in fear of aggregation. Therefore, binding between these proteins could be said to be weak protein-protein interactions, because weak protein-protein interactions are in μM range (Perkins et al. 2010). This means that all the binding affinities measured for these inhibitors in this experiment are weak. When the saturation was not reached the real Kd can be higher and this needs to be kept in mind when applying the information in the results. Graphs on the other hand had very low error bars. All the triplicate tests showed very similar results when compared to each other. This suggests that the individual results are very accurate in this experiment setting.

4.6 In the future

The heterotrimeric structure of PP2A has at least 27 possible changing parts discovered for now. Two different A subunit isoforms, two different C subunit isoforms and 23 different B subunit isoforms and more finds may be on the way. Even from these isoforms PP2A protein could form 92 different trimeric structures (Haesen et al. 2014) In order to conclude how these inhibitors really bind to PP2A, all these subunits should be individually measured. Also, different combinations of the heterotrimeric holoenzyme should be measured in the future. Also, all the other inhibitors found for PP2A, like SET, PME-1 and TIP (Haesen et al. 2012) should be measured by these same means to see where the inhibition happens. In the study of CIP2A, if the protein can ever be purified as whole (Wang et al. 2017), it would be interesting to measure.

5 CONCLUSIONS

Expression and purification protocol for PP2A regulatory B subunit B56 family isoforms proved to work. The binding test results showed that wild type phosphoprotein/α-endosulfin family inhibitors, ARPP19, ARPP16 and ENSA, bound to all these subunits. Inhibition of CIP2A domains was varying, but stronger than other inhibitors studied. Phosphomimicking mutant proteins increased binding affinity for ARPP19 and ARPP16 binding but did not bind to ENSA at all. From these measured subunits, B56ε showed weakest binding and B56δ had the strongest binding. Difference in the similarity of the B56 isoforms may be contributing factor in the way binding occurs. However, many variables need to be taken in account when interpreting these results and as only a part of PP2A B subunit isoforms were studied in this experiment. Further studies are needed to determine how these inhibitors bind to different PP2A isoforms.

ACKNOWLEDGEMENTS

I would like to thank Ulla Pentikäinen, her research group and University of Turku for allowing me to work with them in order to do my master's thesis from the subject that fascinates me. Big thanks also to Jari Ylänne and University of Jyväskylä for helping and preparing me for this final project before graduation.

REFERENCES

Andrade E.C., Musante V., Horiuchi A., Matsuzaki H., Brody A.H., Wu T., Greengard P., Taylor J.R. & Nairn A.C. 2017. ARPP-16 Is a Striatal-Enriched Inhibitor of Protein Phosphatase 2A Regulated by Microtubule-Associated Serine/Threonine Kinase 3 (Mast 3 Kinase). The Journal of neuroscience 37: 2709–2722.

Beresford P.J., Zhang D., Oh D.Y., Fan Z., Greer E.L., Russo M.L., Jaju M. & Lieberman J. 2001. Granzyme A Activates an Endoplasmic Reticulum-associated Caspase-independent Nuclease to Induce Single-stranded DNA Nicks. Journal of Biological Chemistry 276: 43285–43293.

Cho U.S. & Xu W. 2007. Crystal structure of a protein phosphatase 2A heterotrimeric holoenzyme. Nature 445: 53–57.

Ding S., Das S.R., Brownlee B.J., Parate K., Davis T.M., Stromberg L.R., Chan E.K.., Katz J., Iverson B.D. & Claussen J.C. 2018. CIP2A immunosensor comprised of vertically-aligned carbon nanotube interdigitated electrodes towards point-of-care oral cancer screening. Biosensors and Bioelectronics 117: 68–74.

Dulubova I., Horiuchi A., Snyder G.L., Girault J., Czernik A.J., Shao L., Ramabhadran R., Greengard P. & Nairn A.C. 2001. ARPP-16/ARPP-19: a highly conserved family of cAMP-regulated phosphoproteins. Journal of Neurochemistry 77: 229–238.

Gharbi-Ayachi A., Labbé J.-C., Burgess A., Vigneron S., Strub J.-M., Brioudes E., Van-Dorsselaer A., Castro A. & Lorca T. 2010b. The Substrate of Greatwall Kinase, Arpp19, Controls Mitosis by Inhibiting Protein Phosphatase 2A. 330: Science 1673–1677.

Girault J.A., Horiuchi A., Gustafson E.L., Rosen N.L. & Greengard P. 1990. Differential expression of ARPP-16 and ARPP-19, two highly related cAMP-

regulated phosphoproteins, one of which is specifically associated with dopamine-innervated brain regions. Journal of Neuroscience 10: 1124–1133.

Haccard O. & Jessus C. 2011. Greatwall Kinase, ARPP-19 and Protein Phosphatase 2A: Shifting the Mitosis Paradigm. Springer Berlin Heidelberg, Berlin, Heidelberg. Cell Cycle in Development 53: 219-234

Haesen D., Sents W., Ivanova E., Lambrecht C. & Janssens V. 2012. Cellular inhibitors of Protein Phosphatase PP2A in cancer. doi: 10.1111/j.1742-4658.2012.08579.x

Haesen D., Sents W., Lemaire K., Hoorne Y. & Janssens V. 2014. The Basic Biology of PP2A in Hematologic Cells and Malignancies. Frontiers in Oncology 4: 347.

Heron L., Virsolvy A., Peyrollier K., Gribble F.M., Cam A.L., Ashcroft F.M. & Bataille D. 1998. Human α-endosulfine, a possible regulator of sulfonylurea-sensitive KATP channel: Molecular cloning, expression and biological properties. PNAS 95: 8387–8391.

Horiuchi A., Williams K.R., Kurihara T., Nairn A.C. & Greengard P. 1990. Purification and cDNA cloning of ARPP-16, a cAMP-regulated phosphoprotein enriched in basal ganglia, and of a related phosphoprotein, ARPP-19. Journal of Biological Chemistry 265: 9476.

Hunter T. 1991. Protein kinase classification. Methods in Enzymology 200: 3-37

Jerabek-Willemsen M., André T., Wanner R., Roth H.M., Duhr S., Baaske P. & Breitsprecher D. 2014. MicroScale Thermophoresis: Interaction analysis and beyond. 1077: Journal of Molecular Structure 101–113.

Jiang T., Zhao B., Li X. & Wan J. 2016. ARPP-19 promotes proliferation and metastasis of human glioma. NeuroReport 27: 960–966.

Junttila M.R., Puustinen P., Niemelä M., Ahola R., Arnold H., Böttzauw T., Ala-aho R., Nielsen C., Ivaska J., Taya Y., Lu S.-L., Lin S., Chan E.K.., Wang X.-J., Grènman R., Kast J., Kallunki T., Sears R., Kähäri V.-M. & Westermarck J. 2007. CIP2A Inhibits PP2A in Human Malignancies. Cell 130: 51–62.

Kerk D., Templeton G. & Moorhead G.B.G. 2008. Evolutionary Radiation Pattern of Novel Protein Phosphatases Revealed by Analysis of Protein Data from the Completely Sequenced Genomes of Humans, Green Algae, and Higher Plants. Plant Physiology 146: 351–367.

Kumm E.J., Pagel O., Gambaryan S., Walter U., Zahedi R.P., Smolenski A. & Jurk K. 2020. The Cell Cycle Checkpoint System MAST(L)-ENSA/ARPP19-PP2A is Targeted by cAMP/PKA and cGMP/PKG in Anucleate Human Platelets. Cells 9: 472.

Labandera A.-M., Vahab A.R., Chaudhuri S., Kerk D. & Moorhead G.B.. 2015. The mitotic PP2A regulator ENSA/ARPP-19 is remarkably conserved across plants and most eukaryotes. Biochemical and Biophysical Research Communications 458: 739–744.

McConnell J.L., Gomez R.J., McCorvey L.R.A., Law B.K. & Wadzinski B.E. 2007. Identification of a PP2A-interacting protein that functions as a negative regulator of phosphatase activity in the ATM ATR signaling pathway. Oncogene 26: 6021–6030.

Miura K. 2018. An Overview of Current Methods to Confirm Protein-Protein Interactions. doi: 10.2174/0929866525666180821122240

Mochida S. 2014. Regulation of α–endosulfine, an inhibitor of protein phosphatase 2A, by multisite phosphorylation. The FEBS Journal 281: 1159–1169.

Mumby M.C. & Walter G. 1993. Protein serine/threonine phosphatases: structure, regulation, and functions in cell growth. Physiological Reviews 73: 673–699.

Musante V., Li L., Kanyo J., Lam T.T., Colangelo C.M., Cheng S.K., Brody A.H., Greengard P., Le Novère N. & Nairn A.C. 2017. Reciprocal regulation of ARPP-16 by PKA and MAST3 kinases provides a cAMP-regulated switch in protein phosphatase 2A inhibition. 6. doi: 10.7554/eLife.24998

NanoTemper, 2011, Software Manual MO.Control V03_2018-03-14, www.nanotemper-teghnologies.com (accessed on 26.5.2020).

Nooren I.M. & Thornton J.M. 2003. Structural Characterisation and Functional Significance of Transient Protein–Protein Interactions. Journal of Molecular Biology 325: 991–1018.

O'Connor C.M., Perl A., Leonard D., Sangodkar J. & Narla G. 2018. Therapeutic targeting of PP2A. International Journal of Biochemistry and Cell Biology 96: 182–193.

Ogris E., Du X., Nelson K.C., Mak E.K., Yu X.X., Lane W.S. & Pallas D.C. 1999. A Protein Phosphatase Methylesterase (PME-1) Is One of Several Novel Proteins Stably Associating with Two Inactive Mutants of Protein Phosphatase 2A. Journal of Biological Chemistry 274: 14382–14391.

Perkins J.R., Diboun I., Dessailly B.H., Lees J.G. & Orengo C. 2010. Transient Protein-Protein Interactions: Structural, Functional, and Network Properties. Structure 18: 1233–1243.

Puustinen P. & Jäättelä M. 2014. KIAA1524/CIP2A promotes cancer growth by coordinating the activities of MTORC1 and MYC. Autophagy 10: 1352–1354.

Sangodkar J., Farrington C.C., McClinch K., Galsky M.D., Kastrinsky D.B. & Narla G. 2016. All roads lead to PP2A: exploiting the therapeutic potential of this phosphatase. The FEBS Journal 283: 1004–1024.

Seidel S.A., Dijkman P.M., Lea W.A., Bogaart G. van den, Jerabek-Willemsen M., Lazic A., Joseph J.S., Srinivasan P., Baaske P., Simeonov A., Katritch I., Melo F.A., Ladbury J.E., Schreiber G., Watts A., Braun D. & Duhr S. 2013. Microscale thermophoresis quantifies biomolecular interactions under previously challenging conditions. Methods: a Journal for Human Science 59: 301–315.

Seshacharyulu P., Pandey P., Datta K. & Batra S.K. 2013. Phosphatase: PP2A structural importance, regulation and its aberrant expression in cancer. Cancer Letters 335: 9–18.

Thapa C., Roivas P., Haataja T., Permi P. & Pentikäinen U., submitted. Intrinsically disordered PP2A inhibitor proteins ARPP-16/19 interact with PP2A via a two-site mechanism.

Thapa C., unpublished.

Voets E. & Wolthuis R.M.F. 2010. MASTL is the human orthologue of Greatwall kinase that facilitates mitotic entry, anaphase and cytokinesis. Cell cycle 9: 3591.

Wang J., Okkeri J., Pavic K., Wang Z., Kauko O., Halonen T., Sarek G., Ojala P.M., Rao Z., Xu W. & Westermarck J. 2017. Oncoprotein CIP2A is stabilized via interaction with tumor suppressor PP2A/B56. EMBO reports 18: 437–450.

Westermarck J. & Hahn W.C. 2008. Multiple pathways regulated by the tumor suppressor PP2A in transformation. Trends in Molecular Medicine 14: 152–160.

Xu Y., Chen Y., Zhang P., Jeffrey P.D. & Shi Y. 2008. Structure of a Protein Phosphatase 2A Holoenzyme: Insights into B55-Mediated Tau Dephosphorylation. 31: 873–885.

APPENDIX 1. AMINO ACID IDENTITY OF B56 ISOFORMS

Appendix 1. Amino acid sequence identity between B56 isoforms. Darker areas are more similar compared to each other and lighter areas differ more from each other. UniProt codes correspond to each B56 isoform: 2A5A_HUMAN (B56α), 2A5B_HUMAN (B56β), 2A5G_HUMAN (B56γ), 2A5D_HUMAN (B56δ) and 2A5E_HUMAN (B56ε).